Clay Minerals (1984) **19**, 177–193

THE DISTRIBUTION OF OCTAHEDRAL CATIONS IN THE 2:1 LAYERS OF DIOCTAHEDRAL SMECTITES STUDIED BY OBLIQUE-TEXTURE ELECTRON DIFFRACTION

S. I. TSIPURSKY AND V. A. DRITS

Geological Institute of the USSR Academy of Sciences, Pyzhevsky per. 7, Moscow, USSR

(*Received 19 January 1983; revised 26 September 1983*)

ABSTRACT: Olique-texture electron diffraction examination of K-saturated dioctahedral smectites after 70–100 wetting-drying cycles allows the determination of cation distribution between *trans* and *cis* octahedra of the 2:1 layers. Studies of smectites with different compositions has revealed a wide variety of occupancies of the available octahedral sites.

In dioctahedral phyllosilicates only two of the three symmetrically independent octahedral positions are occupied by cations. The 2:1 layer will have a centre of symmetry if the *trans* octahedra are vacant (model 1, Fig. 1a) and it will have none if the cations occupy *trans* octahedral sites as well as *cis* octahedral positions, forming one of the two regular systems of points (model 2, Fig. 1b). Numerous structure refinements of dioctahedral layer-silicates have shown that the octahedral cations occupy only the *cis* octahedral positions of the 2:1 layers if the total number of these cations per unit cell is equal to 4. The probable existence of two-layer micas with non-centrosymmetrical layers was noted by B. B. Zvyagin *et al.* (1979); these authors also specified the possible polytypes of micas with such layers and calculated their diffraction data for ideal models.

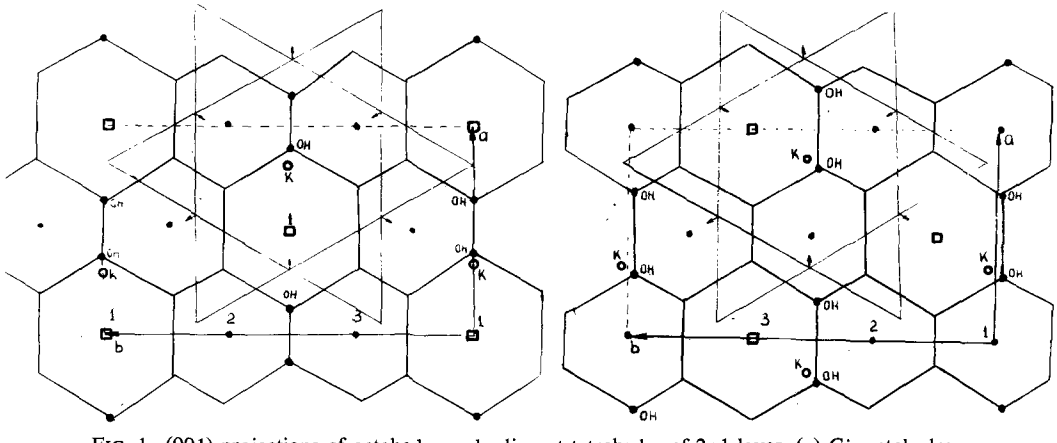

FIG. 1. (001) projections of octahedra and adjacent tetrahedra of 2:1 layer. (a) *Cis* octahedra are occupied (model 1). (b) *Cis* octahedral positions, forming one of the two regular systems of points, are vacant; *trans* octahedra are occupied (model 2).

Based on studies of the hydration properties of montmorillonites from Camp Bertaux and Wyoming, Méring & Glaeser (1954) suggested that the *trans* octahedra of the 2:1 layers of these minerals were occupied by cations. They showed that in the presence of bi-valent interlayer cations this model of the 2:1 layers is favoured due to a better local charge balance (Glaeser & Méring, 1954).

The turbostratic structure of most dioctahedral smectites hinders direct X-ray study of the distribution of the octahedral cations. Méring & Oberlin (1971) approached this problem by analysing the point electron diffraction patterns from microcrystals with the thickness of a single 2:1 layer. They concluded that the structure of the 2:1 layer of Pfaffenreuth nontronite corresponded to model 1 and that of Wyoming montmorillonites to model 2. Subsequent studies using the selected-area electron diffraction method showed that there were beidellites with centrosymmetrical layers and the charge localized in the tetrahedral sheets (Güven *et al.*, 1977) as well as with non-centrosymmetrical layers and the charge equally distributed over the tetrahedra and the octahedra (Besson & Tchoubar, 1972).

This experimental procedure is, however, difficult to carry out and it is also difficult to interpret the point diffraction patterns. First one cannot be sure that the sample thickness represents one single layer. Second, distortions of the intensity distribution are inevitable because of the local deformations of single layers and their structure distortions resulting from the interaction with the beam. Finally, the diffraction data obtained for separate single layers may fail to reflect the octahedral cation distribution in the 2:1 layers forming thicker particles.

Several authors (Goodman *et al.*, 1976; Rozenson & Heller-Kallai, 1977) tried to compensate for the insufficient reliability of the diffraction data by using Mössbauer spectroscopy. It became a tradition to resolve the experimental spectra of the Fe^{3+}-containing smectites, as well as glauconites and celandonites, into two doublets, one of which was related to the Fe^{3+} ions occupying *cis* octahedral positions and the other to the Fe^{3+} ions occupying *trans* octahedral sites. Such an approach was recently found to be erroneous by Daynyak (1980) and Bookin *et al.* (1978, 1979). They showed that one of the necessary conditions for reliable interpretation of Mössbauer spectra of Fe^{3+}-containing phyllosilicates was the availability of data on the cation distribution in the unit cell, averaged over the volume of the crystal.

One of the best ways of determining directly the distribution of the octahedral cations is by utilizing the increase in structural ordering resulting from re-arrangement of layer stacking. Tsipursky *et al.* (1978), using oblique-texture electron diffraction, showed that K-saturation of nontronites led to an increase in structural ordering, which was accompanied by the appearance of distinct reflections with $k \neq 3n$ on the diffraction patterns. Analysis of the intensities of these reflections confirmed the conclusion of Méring & Oberlin (1971) regarding the centrosymmetrical structure of the 2:1 nontronite layers.

Besson (1980), by saturating the samples with Cs and comparing experimental X-ray diffraction curves with those calculated for different models, confirmed that the Rupsroth smectite and beidellite from the Black Jack Mine had 2:1 layers with occupied and vacant *trans* octahedra, respectively.

Mamy & Gaultier (1976) suggested a more effective way of improving the structural ordering of smectites which, in addition to K-saturation, involved a large number of wetting–drying cycles (WD). Besson *et al.* (1982) used this technique to study the Garfield nontronite by several diffraction methods. Comparison of the intensity distributions on the

experimental diffraction patterns with those calculated showed a quantitative fitting, which led to the conclusion that the *trans* octahedral sites of the 2:1 layers of nontronites were vacant. Besson (1980) also confirmed the observation of Méring & Glaeser that the 2:1 layers of the Wyoming montmorillonite were non-centrosymmetrical.

We have used the technique of Mamy & Gaultier (1976) for structural rearrangement of more than 30 samples of dioctahedral smectites of different compositions and genesis. Study of these by oblique-texture electron diffraction has shown that the cation distribution over available octahedral sites in 2:1 dioctahedral smectites varies more than supposed.

TABLE 1. Crystallochemical formulae of the smectites studied on $O_{10}(OH)_2$ basis. Sample details are given below.

Sample number	Nature and amount of cations									
	Interlayer				Tetrahedra		Octahedra			
	Ca	Na	K	Mg	Si	Al	Al	Fe^{3+}	Fe^{2+}	Mg
1	0·22	0·01	0·04		3·95	0·05	1·38	0·18		0·44
2	0·06	0·20			3·96	0·04	1·54	0·18		0·26
3	0·06	0·17	0·09		3·98	0·02	1·38	0·14	0·01	0·48
4	0·13	0·02	0·04		3·91	0·09	1·36	0·39	0·02	0·24
5	0·03	0·31	0·02		4·00		1·51	0·10		0·39
6	0·15	0·01	0·03		4·00		1·40	0·26		0·34
7	0·18	0·05	0·02		3·98	0·02	1·32	0·26		0·41
8	0·06	0·17	0·07		4·00		1·39	0·26	0·05	0·30
9	0·13	0·25			3·83	0·17	1·47	0·19		0·34
10	0·15	0·20	0·10		3·89	0·11	0·89	0·62	0·03	0·46
11	0·11	0·04	0·30		4·00		0·20	1·13	0·38	0·29
12	0·06	0·21	0·27		3·71	0·29	1·64	0·05	0·01	0·31
13	0·10	0·05	0·05	0·27	3·73	0·27	1·05	0·37		0·57
14		0·46‡			3·86	0·14	1·68			0·32
15	0·07	0·01	0·11	0·15	3·41	0·59	1·57	0·37	0·01	0·05
16	0·11	0·03	0·16		3·53	0·47	0·96	0·88	0·02	0·26
17	0·12	0·05	0·01	0·17	3·45	0·55	0·33	1·59		0·08
18	0·23	0·03	0·01		3·49	0·51*		1·87	0·17	
19	0·16	0·03	0·01	0·05	3·65	0·35		1·92		0·08
20		0·02	0·40	0·04	3·46	0·54†	0·15	1·85		

* Fe^{3+} instead of Al in tetrahedral sites.

† Cation composition of tetrahedral sheet is $Si_{3.46}Al_{0.40}Fe^{3+}_{0.14}$.

‡ Sum of interlayer cations obtained by sodium-radioactivity method of G. Besson.

1. Bentonite, Ascan (Drits & Kossovskaya, 1980). 2. Montmorillonite, Wyoming (Mamy & Gaultier, 1976). 3. Bentonite, Ascan (Drits & Kossovskaya, 1980). 4. Hydrothermal alteration product of dacite–andesite, Kunashir Island (Drits & Kossovskay, 1980). 5. Bentonite, Oglanlyn, from Dr V. I. Eirish, Geological Institute, Kazan, USSR. 6, 7. Bentonites, Gumbrin, from Dr V. I. Eirish, Geological Institute, Kazan, USSR. 8. Bentonite, Sarygiukh, from Dr V. I. Eirish, Geological Institute, Kazan, USSR. 9. Ancient soil in sedimentary rocks, Kazakhstan (Drits & Kossovskay, 1980). 10. Clay from Panama Bassin, Pacific Ocean (Drits & Kossovskay, 1980). 11. Modern sediment, Red Sea (Boutouzova *et al.*, 1979). 12. Bentonite, Ascan (Drits & Kossovskay, 1980). 13. Clay from geothermal field, Kamchatka (Drits & Kossovskay, 1980). 14. Beidellite, Rupsroth (Besson, 1980). 15. Clay from geothermal field, Kamchatka (Drits & Kossovskay, 1980). 16. Modern red clay from Pacific Ocean (Tsipursky *et al.*, 1978). 17–19. Weathering crust of gneisses (Tsipursky *et al.*, 1978). 20. Nontronite, Garfield (Besson *et al.*, 1982).

SPECIMEN DESCRIPTION, PREPARATION AND EXPERIMENTAL TECHNIQUE

Dioctahedral smectites differing in ion content, extent of layer charge, charge distribution over octahedral and tetrahedral sheets, and particle morphology were investigated. Crystal-chemical formulae and source data are given in Table 1. X-ray diffraction curves obtained from oriented samples saturated with ethylene glycol and glycerol, and after heating, were used to establish the purity of the samples studied.

All the smectites were K-saturated according to the following technique. The sample was placed in a 1 N solution of K_2CO_3 and held there for 3 h at 70°C. The sample was then washed to remove salt solution. The K-saturated products showed *d*-spacings between 10·2–11·0 Å. The dry K-saturated sample was mixed with distilled water, dried at 80–100°C and then re-wetted; this procedure was repeated 70–100 times. The samples were then studied by oblique-texture electron diffraction. A drop of suspension was placed on a thin collodium film-support. After drying, a highly oriented specimen was obtained. If such a specimen is made up of a set of single crystals with perfect structures then, when inclined relative to the beam, a diffraction pattern will be obtained in which the reflections are distributed over a series of ellipses (Zvyagin, 1967). On the first ellipse the 02*l* and 11*l* reflections are grouped, on the second those with indices 20*l*, 13*l*, etc. The sequence of reflections with different indices that may be expected on the first ellipse of the 1*M* mica pattern is presented schematically in Fig. 2.

The most important advantage of this method compared with powder X-ray diffraction is the possibility of obtaining a two-dimensional distribution of intensities for finely dispersed layer-silicates.

Zvyagin (1967) and Zvyagin *et al.* (1979) demonstrated the effectiveness of this method for revealing various subtle structural features of clay minerals. According to their results, and also to the data obtained by Tsipursky & Drits (1977), it is possible to conclude that

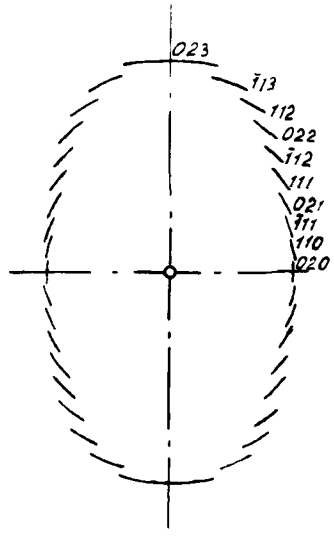

FIG. 2. Arrangement of reflections on the first ellipse of the oblique-texture electron diffraction pattern.

the character of the interaction of electrons with clay particles is purely kinetic. Hence, the intensities of reflections without any dynamic corrections may be used to test the validity of a structural model.

The effectiveness of the oblique-texture method is reduced in the case of smectites because in a vacuum dehydration takes place which changes the initial structure. However, if at the same time a relatively high structural ordering can be achieved, the diffraction data may be used to obtain additional information on the structural features of the 2:1 layers, their azimuthal orientations, etc.

Zvyagin & Pinsker, (1949), and later Zvyagin (1967), demonstrated for the first time by electron diffraction that a high degree of ordering existed in dehydrated (Ascan) montmorillonite and the Black Jack Mine beidellite, for which the unit-cell parameters were determined.

However, electron diffraction has not been used for systematic study of structural features of smectites because most of them appear to have turbostratic structure (Fig. 3a).

Although a large number of smectites have been studied, only three natural Ca-nontronites and the Black Jack Mine beidellite proved to have a sufficiently high degree of ordering in layer stacking. Disordered structures of smectites in the dehydrated state may be attributed to the type of exchangeable cations. Many of the oceanic smectities studied proved to have K in interlayer positions, and their structural ordering in vacuum was higher than that of Ca- or Na-smectites. It may be assumed that when the interlayer water is completely removed, the relatively small Ca, Na and Mg ions are contained within the hexagonal rings of the 2:1 layers and therefore the process of dehydration is accompanied by random interlayer shifts and rotations of the layers at arbitrary angles.

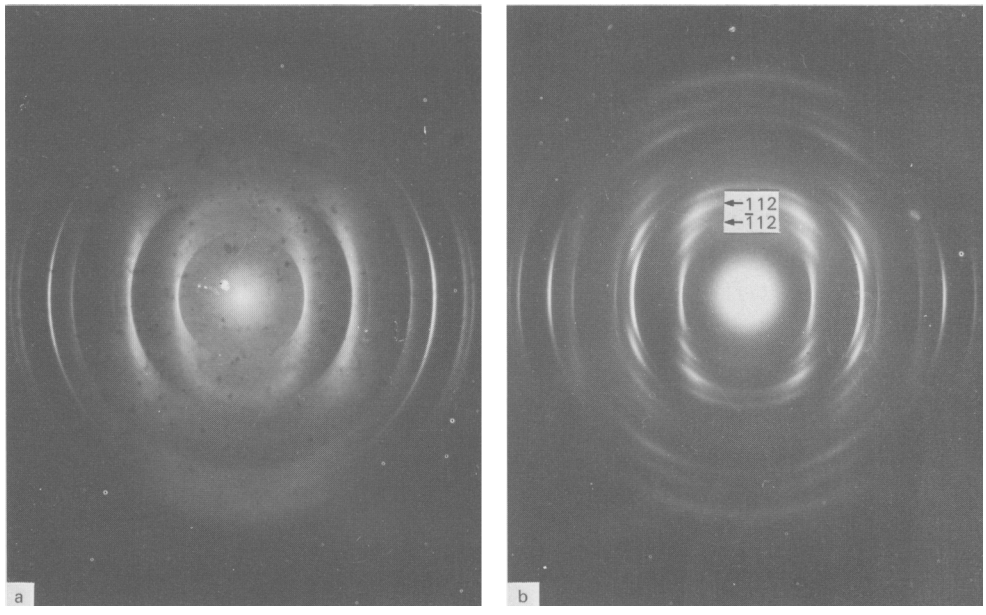

FIG. 3. Oblique-texture electron diffraction patterns of (a) natural smectite with turbostratic structure and (b) Fe^{3+}-montmorillonite (sample 11, Table 1). Angle between the initial electron beam and the normal to the surface of the sample is 60°.

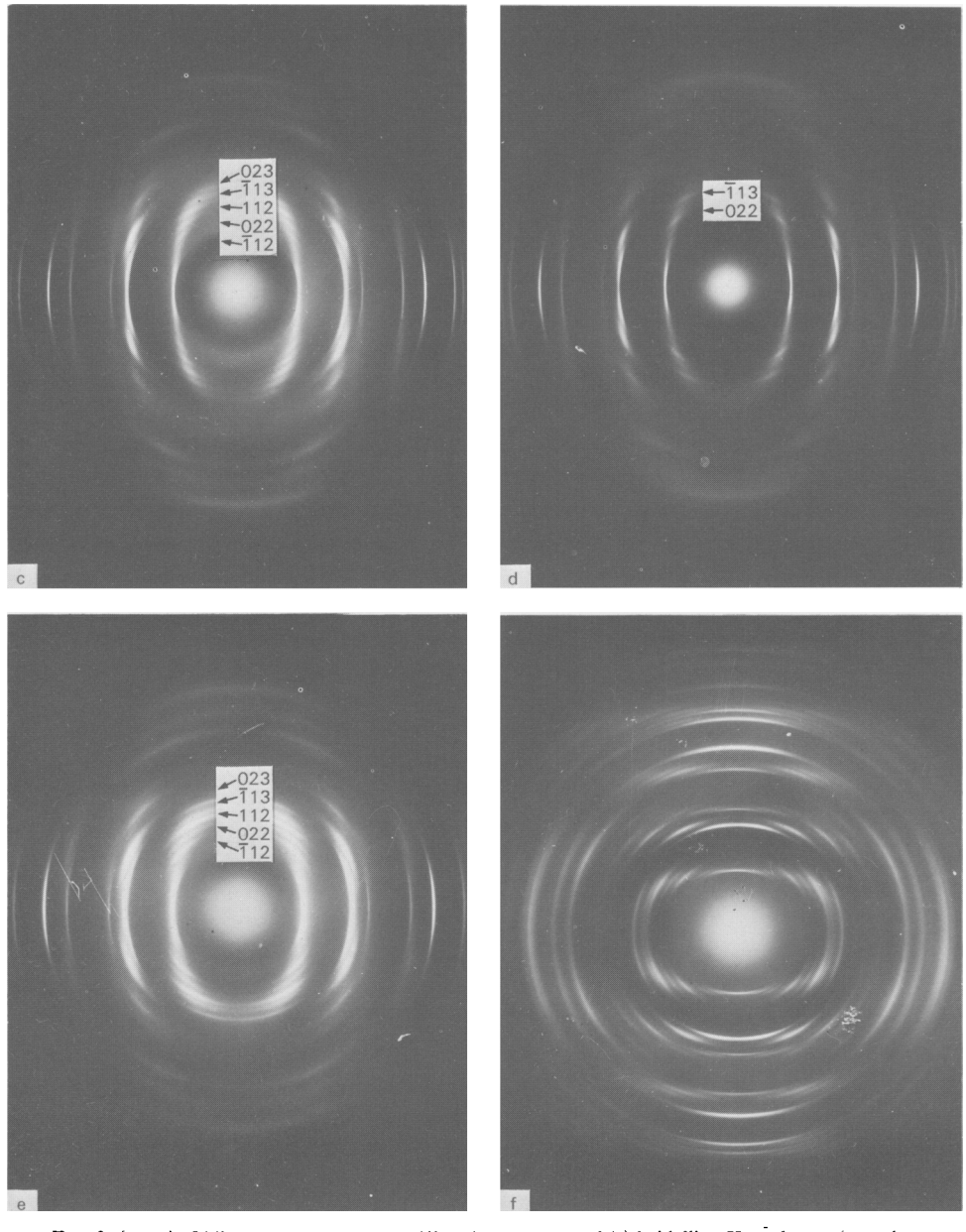

FIG. 3. (cont.) Oblique-texture electron diffraction patterns of (c) beidellite, Kamchatca (sample 15, Table 1), (d) montmorillonite, Wyoming (sample 2, Table 1), (e) clay from Panama Basin (sample 10, Table 1), (f) glauconite from Piltene. Angle between initial electron beam and the normal to the surface of the sample is 60°.

Such effects in the structures of dehydrated Ca- and Na-smectites may also be promoted by the fact that the mica-like stacking mode is not the most favourable because of the electrostatic interaction of the tetrahedral cations of the adjacent layers.

The replacement of Ca and Mg by K in the interlayers leads to an increase in exchangeable cation content and it also favours the elimination of random defects due to the packing of adjacent layers according to the mica-like mode.

ELECTRON DIFFRACTION OF K-SMECTITES

K-smectites without WD cycles

The K_2CO_3 treatment proved to be most effective for nontronites. Initially, they had turbostratic or semi-ordered structures, and after the treatment distinguishable reflections appeared both on the first and second ellipses. The data obtained indicated that all the 2:1 layers in the particles of natural nontronites had the same azimuthal orientation. The replacement of Ca by K in vacuum decreased the number of translational defects. The ribbon-like form of the nontronite single crystals confirmed that rotational defects were absent. Indeed, the rates of crystal growth are not equal along different crystallographic directions, which is due to the essentially different structure of frontal surfaces along each of these directions. If all the layers of the crystal have the same orientation, their growth rates along every given direction will be the same. Consequently, the ribbon-like form of crystals is automatically provided if their growth along some direction, the *a*-axis for example, proceeds more quickly.

It is important to emphasize that with ribbon-like crystals the K_2CO_3 treatment is quite sufficient to produce in a vacuum particles with a mica-like stacking mode of identically oriented layers. The Fe^{3+}-smectites from Red Sea sediments that have ribbon-like particles but, unlike nontronites, with layer charge localized in octahedra, may serve as an example (Fig. 3b).

Electron diffraction study of K-saturated (Al, Mg)-smectites with isometric or poorly shaped particles revealed low structural ordering. On the first ellipse, only continuous diffuse scattering was present, and only on the second ellipse were discreet maxima with $k = 3n$ usually discernible. Such patterns may correspond to structures where packing defects are caused either by random $\pm 120°$ rotations of layers, or by their $\pm b/3$ shifts. It is impossible to give preference to any of the two models without precise analysis of the intensity distribution. However, selected-area electron diffraction indicated that a relatively high concentration of faults caused by rotations of adjacent layers at arbitrary angles was another important reason for low structural perfections of the smectites in question.

K-smectites after 70–100 WD cycles

According to the data of Mamy & Gaultier (1976), the 2:1 layers in particles of smectites after 70–100 WD cycles had either identical azimuthal orientations or were rotated to angles $n60°$.

In the present study, increase in the number of WD cycles led to more distinguishable 11*l* and 02*l* reflections on the first ellipse with a small redistribution of intensities on the second one. After 70–100 WD cycles the patterns of most smectites had distinguishable reflections on the first and the second ellipses (Fig. 3c,d,e), the general quality of the diffraction pattern being similar, for example, to that of glauconite (Fig. 3f).

These experimental data allow us to conclude that after 70–100 WD cycles most of the 2:1 layers in the particles of the majority of K-smectites have identical azimuthal

orientations. This implies that the existence of semi-ordered structures in K-smectites that have not been subjected to WD cycles is caused mainly by $\pm b/3$ shift defects, as it seems highly improbable that during the WD procedure mutual $\pm 60°$ or $\pm 120°$ rotations of layers may take place. It follows, therefore, that the WD procedure eliminates defects mainly caused by azimuthal rotations of layers at angles of a relatively small range of $\pm(0–30°)$*.

Analysis of the geometry of the reflections and their indices indicated that the smectites studied had monoclinic one-layer unit cells similar to those of 1*M* micas, with the parameters listed in Table 2. It is evident from this Table that all (Al, Mg)-smectites (beidellites and montmorillonites) may be divided into three groups according to the values of $c \cdot \cos \beta$. In the first group, $c \cdot \cos \beta$ is considerably greater than $a/3(0{\cdot}37a \div 0{\cdot}38a)$, in the second group it is near to $a/3(0{\cdot}34a \div 0{\cdot}35a)$, while in the third it is equal to or less than $a/3$. The intensity distribution on the first ellipse is similar for (Al, Mg)-smectites from the same group, but differs noticeably for smectites from different groups. A marked difference is observed for smectites with maximum and minimum $c \cdot \cos \beta$ values. For instance, the strongest reflections on the patterns of (Al, Mg)-smectites from the first group with the maximum $c \cdot \cos\beta = -0{\cdot}38a$ are $\bar{1}12$ and 112, and between them there is a weak 022 reflection.

TABLE 2. Unit-cell parameters and occupancies of the *trans* octahedral sites (P_t%) of the smectites studied.

Sample number	a (Å)	b (Å)	c (Å)	β (°)	$\frac{-c \cdot \cos \beta}{a}$	P_t (%)
1	5·18	8·97	10·07	99·6	0·32	75–100
2	5·18	8·98	10·10	99·5	0·32	75–100
3	5·18	8·97	10·05	100·4	0·35	50–75
4	5·18	8·98	10·08	101·5	0·38	0–25
5	5·18	8·98	10·10	99·5	0·32	75–100
6	5·19	9·00	10·10	101·3	0·38	0
7	5·19	9·00	10·10	101·3	0·38	0
8	5·18	8·97	10·20	101·3	0·38	0
9	5·18	8·98	10·13	99·8	0·33	75–100
10	5·18	8·98	10·08	101·0	0·37	25–50
11	5·23	9·06	10·20	100·3	0·35	0
12	5·18	8·98	10·05	101·4	0·38	0
13	5·18	8·97	10·10	100·5	0·35	50–75
14	5·18	8·98	10·10	99·6	0·32	75–100
15	5·18	8·98	10·08	100·2	0·34	50–75
16	5·20	9·01	10·20	101·3	0·38	0
17	5·26	9·12	10·10	101·0	0·37	0
18	5·29	9·17	10·10	101·0	0·36	0
19	5·26	9·12	10·14	101·0	0·37	0
20	5·28	9·14	10·14	100·7	0·36	0

* We assume that after the WD cycles the crystals of the smectites studied may contain up to 30% of the stacking faults due to rotation of adjacent layers by $\pm 120°$. The diffraction characteristics calculated by us for such defect structures show that such a concentration does not change considerably the relative reflection intensitity distribution on the first ellipse.

On the diffraction patterns of the (Al, Mg)-smectites with minimum $c \cdot \cos \beta$ values, the 022 reflection is, in contrast, the strongest and the $\bar{1}12$ and 112 reflections are weak. The intensity of the $\bar{1}13$ reflection increases markedly. On the patterns of the smectites with $c \cdot \cos \beta$ approximately $-(0{\cdot}34a \div 0{\cdot}35a)$, the intensities of the reflections are practically equal.

Smectites with high octahedral Fe^{3+} contents ($Fe^{3+}/Al > 0{\cdot}9$) have similar intensity distributions on the first ellipse, $\bar{1}12$ and 112 being the most intense reflections. The $c \cdot \cos \beta$ values range from $-0{\cdot}35a$ for Fe-smectites (sample 11) to $-(0{\cdot}36a \div 0{\cdot}37a)$ for nontronites. In sample 16, which shows a relatively high octahedral Al content ($Fe^{3+}/Al = 0{\cdot}91$), $c \cdot \cos \beta = -0{\cdot}38a$. The decrease of $c \cdot \cos \beta$ in the case of nontronites is expected as the ionic radius of Fe^{3+} is greater than that of Al^{3+}, which reduces the difference between the sizes of *cis* and *trans* octahedra of 2:1 layers. As a consequence, the shift between the upper tetrahedral sheet and the lower one within the 2:1 layer is closer to $-a/3$ in nontronites than in montmorillonites and beidellites*.

The patterns of the Red Sea Fe-montmorillonite (sample 11, Tables 1 and 2), Wyoming montmorillonite (sample 2, Tables 1 and 2), Kamchatka beidellite (sample 15, Tables 1 and 2) and Panama montmorillonite (sample 10, Tables 1 and 2) that are typical representatives of the different groups are presented in Fig. 3(b,c,d,e). The distribution of intensities in Fig. 3(e) is intermediate between those of Fig. 3(b) and Fig. 3(c).

The data imply that a series of $c \cdot \cos \beta$ values from $-0{\cdot}38a$ to $-0{\cdot}32a$ is possible for (Al, Mg)-smectites with continuous transfers in the intensity distribution between the extreme cases indicated.

It should be noted that approximately 30% of the smectites under study did not undergo any noticeable rearrangement after the WD procedure. Only reflections with $k = 3n$ were registered on their diffraction patterns. In conditions of K-fixation and elimination of stacking defects, such patterns indicated that there were random $\pm 120°$ rotations of the 2:1 layers in the structure of these smectites. These samples are excluded from the following discussion and their characteristics are not included in Table 1.

DISCUSSION

In the general case, the change location and the intensity distribution of $11l$ and $02l$ reflections on the diffraction patterns of the above K-smectites should depend on their chemical composition, the distribution of octahedral cations over *cis* and *trans* octahedral sites, real distortions of the 2:1 layers, and their stacking sequence. In order to evaluate the role of the main factors affecting the diffraction characteristics of K-smectites, we should first consider in more detail the structural features of the 2:1 layers when:

1. Only *cis* octahedral positions are occupied by cations: layer symmetry $C2/m$ (model 1).
2. *Cis* octahedral sites belonging to one regular system of points are vacant: layer symmetry $C2$ (model 2);
3. All the octahedral sites are occupied with the probability of 2/3; the symmetry of a unit cell of the 2:1 layer is $C2/m$ (model 3).
4. The cation distribution is intermediate between the three extreme cases indicated.

As direct determination of the atomic coordinates by diffraction methods for dispersed minerals with defect structures is impossible, we used the method of structural modelling.

* See below the discussion of interlayer shifts in relation to the nature of 2:1 layer distortions.

This allowed us to calculate the parameters which determine the main features of the real structure of the mineral on the basis of the chemical composition, lateral dimensions and the form of unit cell, and then to obtain the atomic coordinates.

To characterize 1*M* dioctahedral micas with vacant *trans* octahedra (model 1), determination of the following parameters is sufficient in the first approximation:

d_o, d_t mean cation–anion bond lengths in octahedra and tetrahedra, respectively;
t_r mean length of the roof edges in *cis* octahedra;
t_n and t_m mean lengths of the edges shared by two *cis* octahedra and by a *cis* and *trans* octahedron, respectively;
h_o, h_t mean thickness of the octahedral and the tetrahedral sheets, respectively;
ε rotation angle of the upper and lower oxygen triads of the octahedra;
ψ octahedral flattening angle;
l_b mean basal tetrahedral edge length;
l_a mean apical tetrahedral edge length;
α tetrahedral rotation angle;
b_t the measurements of the tetrahedral sheet with $\alpha = 0$;
r(K–O) mean distance between K and the surrounding oxygen atoms in the interlayer;
η interlayer thickness.

If these parameters are known it is not difficult to estimate the atomic coordinates which would be closer to those of the real structure of the 2:1 layers than to those obtained from the model formed by regular polyhedra.

To determine the parameters listed above one may make use of the following:

$$d_o = \sum_i C_i d_i (R_i - \mathrm{O});$$

$d_t = 1{\cdot}61x + 1{\cdot}75\,(1-x)$—for cation composition $(\mathrm{Si}_x\mathrm{Al}_{1-x})$;

$$t_n = 0{\cdot}86 t_m = (4d_o^2 - b^2/3)^{0{\cdot}5};$$

$$4\sqrt{2}d_o = 2t_r + t_n + t_m;$$

$$b = 2\sqrt{3}t_r \cos(30^\circ - \varepsilon);$$

$$d_o^2 = \frac{t_r^2}{3} + \frac{h_o^2}{4} = \frac{t_r^2 \cos^2(30^\circ + \varepsilon)}{3} + \frac{t_m^2}{4};$$

$$\sin\psi = \frac{t_r}{\sqrt{3}d_o};\quad 2\sqrt{2/3}\,d_t = \frac{l_a + l_b}{2} = 1{\cdot}01 l_b;\quad b_t = 2\sqrt{3}\,l_b;$$

$$\alpha = \arccos(b/b_t);\quad \eta = c \cdot \sin\beta - 2h_t - h_o;$$

$$r(\mathrm{K-O}) = \left[\frac{\eta^2}{4} + \frac{b^2}{36}(\sqrt{3} - \tan\alpha)^2\right]^{0{\cdot}5}$$

where C_i is the relative content of the cation R_i in the *cis* octahedron with the bond length d_i (R_i–O). It was assumed that the mean bond length R–(O, OH) was 1·93, 1·99, 2·08 and 2·12 Å for Al, Fe^{3+}, Mg and Fe^{2+}, respectively. Most of the formulae listed above are known (Donnay *et al.*, 1964; Radoslovich & Norrish, 1964; Drits, 1969, 1975), and the relations between t_n, t_m and l_b, l_a were obtained empirically from comparison of results from structure refinements of dioctahedral (Al, Mg)-micas. Table 3 (column 2) shows that

TABLE 3. Main structural parameters of dioctahedral micas.

	Phengite 1*M* (Tsipursky & Drits, 1977)		Muscovite $2M_1$ (Güven, 1971)		Muscovite 1*M* (Zvyagin *et al.*, 1979)		Phengite $2M_1$ (Güven, 1971)		Paragonite $2M_1$ (Radoslovich *et al.*, 1964)	
	1	2	1	2	1	2	1	2	1	2
d_t	1·626	1·63	1·643	1·64	1·624	1·62	1·622	1·62	1·651	1·65
l(lat)	2·677	2·69	2·711	2·70	2·671	2·67	2·686	2·67	2·713	2·72
l(bas)	2·631	2·63	2·657	2·65	2·623	2·62	2·625	2·62	2·680	2·67
α^0	8·63	8·7	11·7	11·0	9·33	9·4	6·0	5·1		15·6
h_t	2·207	2·22	2·245	2·24	2·196	2·21	2·22	2·22		2·26
d_o	1·947	1·95	1·930	1·93	1·939	1·94	1·956	1·95	1·913	1·91
t_r	2·808	2·81	2·810	2·82	2·815	2·80	2·842	2·84		2·78
t_n	2·481	2·48	2·427	2·42	2·469	2·48	2·497	2·48	2·417	2·40
t_m	2·932	2·91	2·881	2·85	2·879	2·88	2·885	2·88	2·807	2·82
h_o	2·157	2·16	2·087	2·07	2·113	2·14	2·12	2·11		2·07
ψ^0	56·4	56·3	57·20	57·5	56·95	56·4	57·0	57·1		57·2
ε^0	7·76	7·6	7·84	7·2	6·9	7·3	6·6	6·7		7·6
η	3·395	3·37	3·393	3·42	3·399	3·36	3·36	3·37		3·06
r (K–O)	2·917	2·90	2·857	2·87	2·897	2·87	2·97	2·98	2·641	2·64

1—refinement structure.
2—model.

TABLE 4. Atomic coordinates for different structural models of smectites having the composition of Ascan smectite (sample 12).

	Model 1			Model 2			Model 3		
Atoms	*x/a*	*y/b*	*z/c*	*x/a*	*y/b*	*z/c*	*x/a*	*y/b*	*z/c*
*M*1	0·0	0·0	0·0	0·0	0·0	0·0	0·0	0·0	0·0
*M*2	0·0	0·333	0·0	0·0	0·321	0·0	0·0	0·333	0·0
*M*3	0·0	0·667	0·0	0·0	0·654	0·0	0·0	0·667	0·0
*T*1	0·417	0·329	0·270	0·432	0·333	0·270	0·427	0·333	0·270
*T*2	0·417	0·671	0·270	0·432	0·662	0·270	0·427	0·667	0·270
K	0·5	0·0	0·5	0·5	0·0	0·5	0·5	0·0	0·5
O1	0·481	0·5	0·320	0·489	0·496	0·335	0·487	0·5	0·330
O2	0·172	0·728	0·335	0·173	0·725	0·335	0·172	0·728	0·330
O3	0·172	0·272	0·335	0·170	0·268	0·320	0·172	0·272	0·330
O4	0·419	0·0	0·105	0·334	−0·024	0·105	0·369	0·0	0·108
O5	0·348	0·691	0·110	0·417	0·656	0·109	0·369	0·667	0·108
O6	0·348	0·309	0·110	0·343	0·347	0·109	0·369	0·333	0·108

the basic features of the real (Al, Mg)-mica structures may be satisfactorily predicted with the help of the formulae listed above.

We used these formulae to determine the bond lengths and, subsequently, the atomic coordinates of the K-saturated (Al, Mg)-smectites with vacant *trans* octahedra (model 1)*. As an example, the atomic coordinates calculated for the Ascan smectite (sample 12) are presented in Table 4.

* The structural and diffraction features of nontronites have been described in detail by Besson *et al.* (1982).

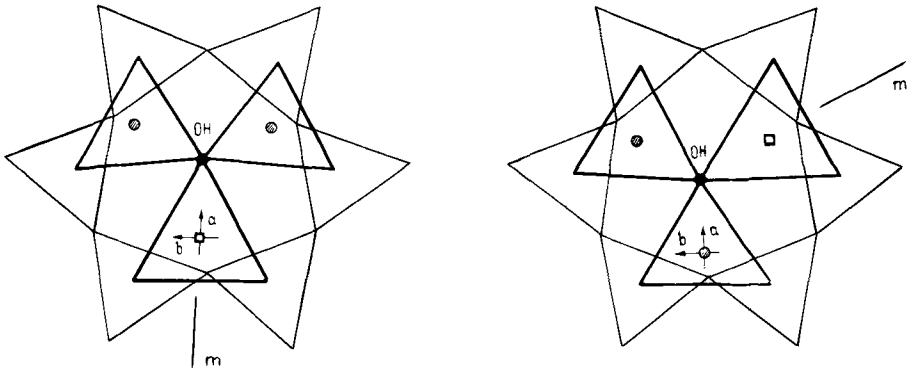

FIG. 4. (001) projections of the upper oxigen triads of the octahedra and adjacent tetrahedra: (a) model 1; (b) model 2.

For the same chemical composition of tetrahedra, octahedra and interlayers, one may assume that in the octahedral sheets of centrosymmetrical and non-centrosymmetrical layers similar structural distortions occur that predetermine the basic structural features of these layers. Thus it is possible to suggest the following simple way of determining atomic coordinates for the structure with $C2$ layers.

Consider the fragments of structural models 1 and 2 (Fig. 1), in particular that representing the (001) projections of the upper and oxygen triads of the octahedra and the adjacent tetrahedra (Fig. 4). It may be seen that the m symmetry plane of the half-layer in model 1 is rotated 120° relative to the m symmetry plane of the half-layer of model 2.

Thus if the atomic coordinates for the upper half-layer of model 1 are known, its 120° rotation will provide atomic coordinates for the half-layer of model 2 relative to new a and b axes. The coordinates of the remaining atoms are obtained by rotation of the half-layers around b (Fig. 5). Atomic coordinates for model 3 are obtained by averaging atomic

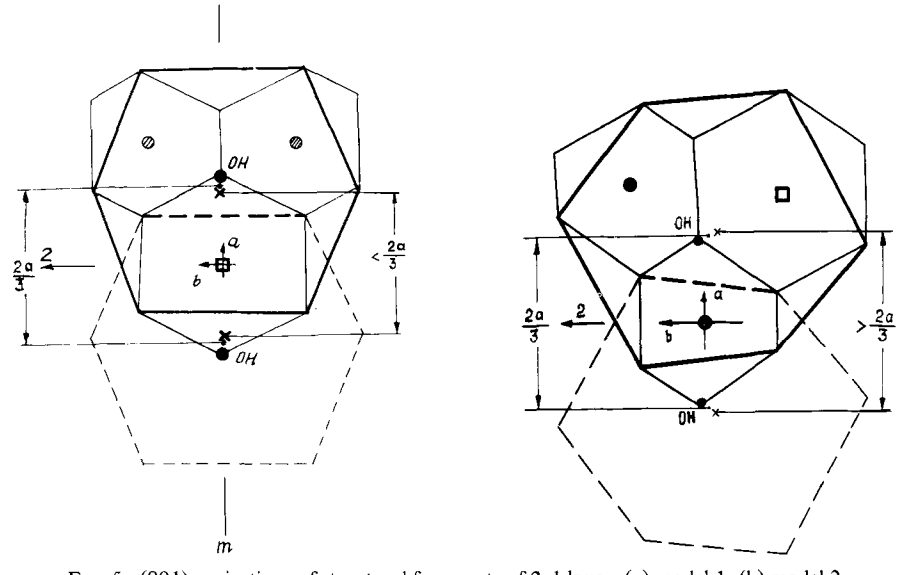

FIG. 5. (001) projections of structural fragments of 2:1 layer: (a) model 1; (b) model 2.

coordinates for models 1 and 2 to make the sizes of all octahedra equal. Coordinates derived in this way for structures of the same composition as Ascan smectite (sample 12) with octahedral cations distributed as in models 1, 2 and 3 are given in Table 4.

In models 1 and 2, the value of $c \cdot \cos \beta$ is determined by mutual shifts of the octahedral and tetrahedral sheets within the 2:1 layer and by relative shifts of the centres of the ditrigonal rings of the adjacent tetrahedral sheets. If the latter is absent or inconspicuous the value of $c \cdot \cos \beta$ is determined by the structural features of the 2:1 layers (Bailey, 1966). In the 2:1 layer formed by regular polyhedra, the centres of the hexagonal rings of the upper tetrahedral sheet are shifted $2a/3$ relative to the centres of the lower sheet. In real structures, as it is seen in Fig. 5, counter-rotation of the upper and lower oxygen triads of octahedra due to the electrostatic interaction of cations determines the shift of the centres of the rings of the upper and lower tetrahedral sheets, which is less than $2a/3$ for vacant trans-octahedra and more than $2a/3$ for vacant *cis*-octahedra. Hence when a noticeable interlayer shift is absent, the relations $c \cdot \cos \beta > a/3$ and $c \cdot \cos \beta < a/3$ must be valid for models 1 and 2 respectively. Apparently, the greater the difference in the size of vacant and occupied octahedra, the greater the deviation of the intralayer displacement from $a/3$.

For the Ascan smectite (sample 12, Tables 1 and 2), the experimental value of the interlayer shift $c \cdot \cos \beta = -0{\cdot}38a$ is equal to the sum of the intralayer shift ($-0{\cdot}37a$) and the shift of the nearest tetrahedral sheet of the adjacent layers ($-0{\cdot}01a$). After atomic coordinates for model 2 were obtained as indicated above, the two components mentioned appeared to be $-0{\cdot}315a$ and $0{\cdot}007a$, and the resulting interlayer shift was therefore $-0{\cdot}308a$. Thus even geometrical analysis of the diffraction patterns of K-smectites may prove sufficient for conclusions to be drawn regarding occupancies of the *trans* and *cis* octahedra. Note that the sequence of reflections on the second ellipse with indices $\bar{2}0(l+1)$, $13l$, $\bar{1}3(l+1)$, $20l$ on the pattern of a mineral with $c \cdot \cos \beta > a/3$, will change to $13l$, $\bar{2}0(l+1)$, $20l$, $\bar{1}3(l+1)$ in the case of minerals with $c \cdot \cos \beta < a/3$.

TABLE 5. $\phi_{calc.}$ (02l) and $\phi_{calc.}$ (11l) for models of smectites with different octahedral cation distributions.

hkl	1	2	3	4	5	6
020	840	690	240	140	160	140
110	20	50	100	140	270	400
$\bar{1}11$	350	250	60	10	60	100
021	60	30	20	20	60	90
111	—	10	60	90	160	260
$\bar{1}12$	580	480	470	430	430	320
022	170	230	420	530	590	730
112	630	540	530	480	470	360
$\bar{1}13$	130	170	230	370	380	480
023	210	170	180	200	210	160
113	10	20	40	100	90	120
$\bar{1}14$	10	—	10	10	10	10

Columns 1–6 correspond to the following cation occupancies of the *trans*, *cis*-1 and *cis*-2 octahedral sites. (1) 0·0; 1·0; 1·0 (model 1). (2) 0·25; 0·75; 1·0. (3) 0·5; 0·5; 1·0. (4) 0·67; 0·67; 0·67 (model 3). (5) 0·85; 0·25; 1·0. (6) 1·0; 0·0; 1·0 (model 2).

For models of the same composition as Ascan smectite (sample 12), but with different variants of cation distribution over octahedral sites, we have calculated structural factors ϕ^2 (*hkl*) for the 02*l*, 11*l*, 20*l* and 13*l* reflections. The intensities of 11*l* and 02*l* reflections appeared to be most sensitive to the changes in cation distribution (Table 5). The gradual transfer from model 1 to model 3 leads to a decrease in intensities of the strongest 020, $\bar{1}12$

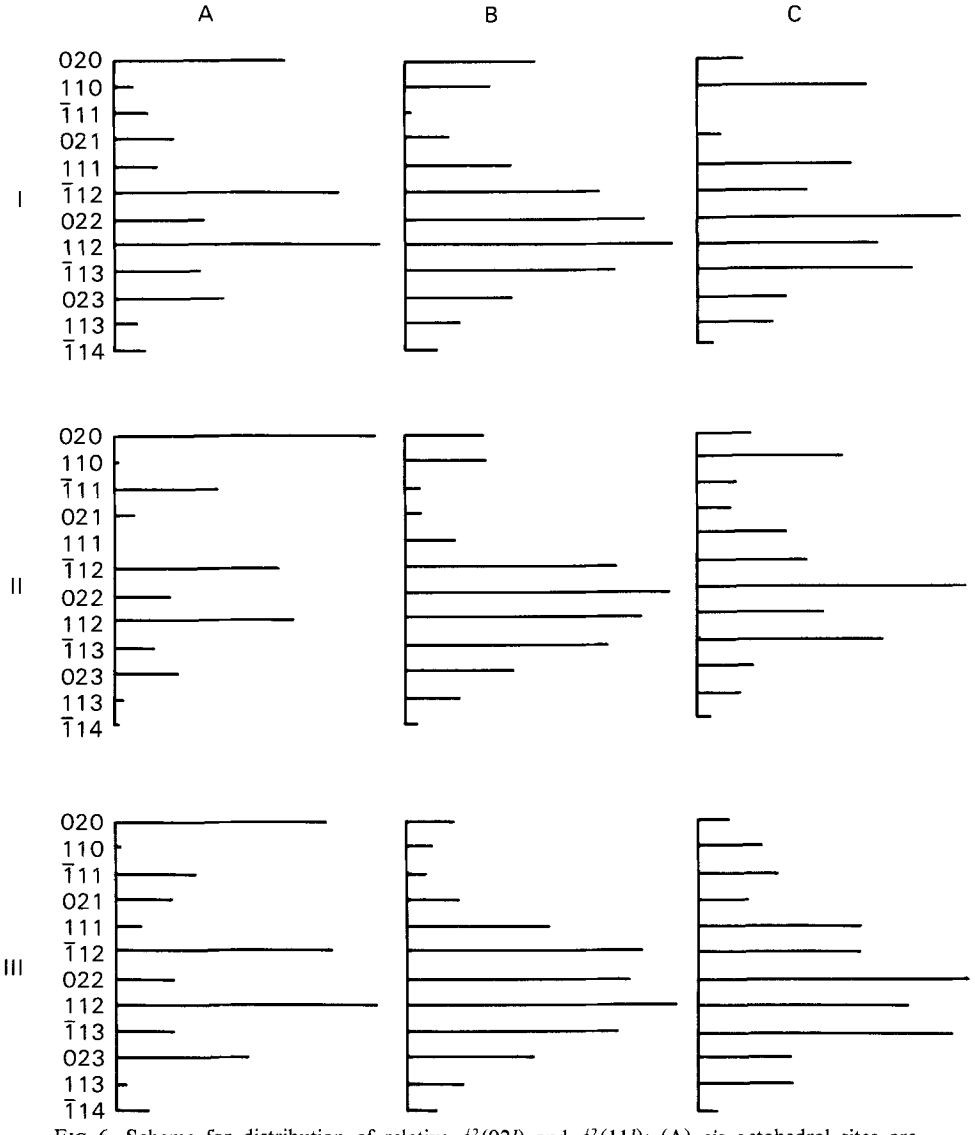

FIG. 6. Scheme for distribution of relative $\phi^2(02l)$ and $\phi^2(11l)$: (A) *cis* octahedral sites are occupied, *trans* octahedral sites are vacant (model 1); (B) all octahedral sites are occupied with equal probability (model 3); (C) *trans* octahedral sites and one of the symmetrical independent *cis* octahedral sites are occupied (model 2). I—(Al,Mg)-smectite without any distortions of structural polyhedra ('ideal' model). II—(Al,Mg)-smectite with distortions of 2:1 layers. III—Nontronite with the distortions of 2:1 layers.

and 112 reflections and an increase in intensities of the weaker $\bar{1}13$ and 022 reflections. With the equally probable cation distribution over octahedral sites, the calculated intensities for the whole group of these reflections are 'equalized'. With the transfer from model 3 to model 2, the $\bar{1}12$, 112 and 023 reflections are weakened, and the 022 and $\bar{1}13$ reflections appear to be the strongest.

To evaluate the influence of structural distortions of the 2:1 layers on the $11l$ and $02l$ intensities for each of the patterns, ideal structural models were constructed using undistorted polyhedra and $\alpha^\circ = \varepsilon^\circ = 0$ were considered. The chemical composition corresponded to that of sample 12. $\phi^2(02l)$ and $\phi^2(11l)$ were calculated for each model and their relative values for the three extreme cases of the cation distribution are presented in Fig. 6.

In order to evaluate the influence of cation composition of octahedra, $\phi^2(02l)$ and $\phi^2(11l)$ were calculated for nontronite (sample 20) taking account of the real distortions of 2:1 layers that may be expected for these minerals (Besson *et al.*, 1982). Relative values of $\phi^2(02l)$ and $\phi^2(11l)$ obtained for nontronite with the same chemical composition as Garfield nontronite (sample 20, Tables 1 and 2) for the three extreme cases of cation distribution are presented in Fig. 6.

Comparison of the data obtained shows that the dominant factor determining the main features of the $02l$ and $11l$ reflection intensity is the distribution of octahedral cations over *cis* and *trans* positions. The specific cation composition of the 2:1 layers and their structural distortions affect mainly the absolute intensity values and not their relative distribution. Analysis of the variations of $\phi^2(02l)$ and $\phi^2(11l)$ taking account of the above factors shows that the cation distribution over the available octahedral sites may be established using the data presented in Table 5 and in Fig. 6, based on the comparison of calculated and experimental intensities.

As the intensities have been estimated visually on the basis of a comparison of diffraction patterns of the same sample with resolvable exposures, the accuracy of the determination of occupancies does not exceed 20%.

From Table 2 it is clear that a wide variety of cation distribution modes over *cis* and *trans* octahedra is observed in dioctahedral smectites.

It may be noted that *trans* octahedra tend to be occupied in montmorillonites with the charge localized only in octahedra, whereas centrosymmetric layers are characteristic of smectites with the charge localized in tetrahedra. Montmorillonites from Wyoming (sample

TABLE 6. Comparison of $\phi_{calc.}$ ($02l$, $11l$) and $\phi_{calc.}$ ($02l$, $11l$) for smectites with different occupancies of *trans* octahedral sites (P_t).

hkl	$P_t = 0{\cdot}0$ sample 12		$P_t = 0{\cdot}67$ sample 15		$P_t = 1{\cdot}0$ sample 2	
111	—	—	90	60	260	180
$\bar{1}12$	580	530	430	490	320	320
022	170	200	530	550	730	800
112	630	660	480	490	360	320
$\bar{1}13$	130	130	370	330	480	540
023	210	200	200	220	160	160
113	10	—	100	60	120	80

2), Ascan (sample 1), Kazakhstan (sample 9), Oglanlin (sample 5) and Rupsroth (sample 14) that have almost fully occupied *trans* octahedra may serve as an example. The Black Jack Mine beidellite (Zvyagin, 1967), Ascan beidellite (sample 12) and nontronites with tetrahedral charge have vacant *trans* octahedra. The typical beidellites from Kamchatka (samples 13 and 15) have random cation distribution.

On the other hand, only *cis* octahedral sites are occupied in the high-charge ferric montmorillonite from the sediments of the Red Sea (sample 11), as well as in Gumbrin and Sarygiukh montmorillonites (samples 6, 7 and 8). Random cation distribution is found in the typical Ascan montmorillonite (sample 3).

It is interesting to note that smectites from the same deposit with very close chemical composition may have totally different octahedral cation distributions (samples 1, 3 and 12, Tables 1 and 2).

ACKNOWLEDGMENTS

The authors thank referees for detailed comments on an earlier version of this paper.

REFERENCES

BAILEY S.W. (1966) The status of clay mineral structures. *Clays Clay Miner.* **14,** 1–23.

BESSON G. (1980) *Structure des smectites dioctahedrique, parametres conditionnant les fautes d' empilement des feuillets.* Thèse de Doctorat d'etat et Sciences Physiques, Orléans.

BESSON G. & TCHOUBAR C. (1972) Détérmination du group de symmétrie du feuillet élémentaire de la beidellite. *C.R. Acad. Sci. Paris* **275,** 633–636.

BESSON G., DE LA CALLE C., RAUTUREAU M., TCHOUBAR C., TSIPURSKY S.I. & DRITS V.A. (1982) X-ray and electron diffraction study of the structure of the Garfield nontronite. *Proc. Seventh Int. Clay Conf., Bologna and Pavia.* 29–40.

BOOKIN A.S., DAINYAK L.G. & DRITS V.A. (1978) Interpretation of the Mössbauer spectra of layer silicates on the basis of the structural modelling. *Phys. Chem. Miner.* **3,** 58–59.

BOOKIN A.S., DAINYAK L.G. & DRITS V.A. (1979) Interpretation of the Mössbauer spectra of Fe^{3+}-containing layer silicates on the basis of the structural modelling. Pp. 23–41 in: *Cation Ordering in Structures of Minerals* (L. I. Lapides, editor). Nauka, Novosibirsk.

BOUTOUZOVA G.YU., DRITS V.A., LISITSINA N.A. & TSIPURSKY S.Y. (1979) The dynamics of the formation of clay minerals in ore-bearing sediments of the Atlantis II (Red Sea) (in Russian). *Litologiya i poleznye iskopaemye* **1,** 20–42.

DAINYAK L.G. (1980) *The interpretation of the Mössbauer spectra of some Fe^{3+}-containing silicates on the basis of structural modelling* (in Russian). Thesis, Geological Institute, Academy of Sciences, Moscow.

DONNAY G., DONNAY J.D.H. & TAKEDA H. (1964) Trioctahedral one-layer micas. II. Prediction of the structure from composition and cell dimension. *Acta Cryst.* **17,** 1374–1377.

DRITS V.A. (1969) Some general remarks on the structure of trioctahedral micas. *Proc. Int. Clay Conf., Tokyo,* 51–59.

DRITS V.A. (1975) Structural and crystal-chemical features of layer silicates. Pp. 32–35 in: *Crystal Chemistry of Minerals and Geological Problems* (A. G. Kossovskaya, editor). Nauka, Moscow.

DRITS V.A. & KOSSOVSKAYA A.G. (1980) Geological crystal chemistry of rock-forming dioctahedral smectites. *Litologiya i poleznye iskopayemye* **1,** 84–112.

GLAESER R. & MÉRING J. (1954) Isothermes d'hydration des montmorillonites biioniques (Na,Ca). *Clay Miner. Bull.* **2,** 188–190.

GOODMAN B.A., RUSSELL J.D. & FRASER A.R. (1976) A Mössbauer and IR spectroscopic study of the structure of nontronite. *Clays Clay Miner.* **24,** 53–59.

GUGGENHEIM S. & BAILEY S.W. (1975) Refinement of the margarite structure in subgroup symmetry. *Am. Miner.* **60,** 1023–1029.

GÜVEN N. (1971) The crystal structure of 2M phengite and $2M_1$-muskovite. *Z. Krist.* **134,** 487–490.

GÜVEN N., PEASE R.W. & MURR L.E. (1977) Fine structure in the selected area electron diffraction patterns of beidellite. *Clay Miner.* **12,** 67–74.

MAMY J. & GAULTIER J.P. (1976) Les phenomènes de diffraction de rayonnements X et électronique per les reseaux atomiques: application à l'étude de l'ordre cristalline dans les miréraux argileux. *Ann. Agronomiques* **27,** 1–16.

MÉRING J. & GLAESER R. (1954) Sur le rôle de la valence de cations échangeables dans la montmorillonite. *Bull. Soc. Fr. Miner. Crist.* **77,** 519–522.

MÉRING J. & OBERLIN A. (1971) Smectite. Pp. 193–229 in: *The Electron-Optical Investigation of Clays* (J. A. Card, editor). Mineralogical Society, London.

RADOSLOVICH E.W. & NORRISH K. (1962) The cell dimensions and symmetry of layer-lattice silicates. I. Some structural considerations. *Am. Miner.* **47,** 599–616.

RADOSLOVICH E.W. & BURNHAM C.W. (1964) Crystal structure of coexisting muscovite $2M_1$ and paragonite $2M_1$. *Carnegie Inst. Year Book* **63,** 232–234.

ROZENSON I & HELLER-KALLAI I. (1977) Mössbauer spectra of dioctahedral smectites. *Clays Clay Miner.* **25,** 94–101.

TSIPURSKY S.I. & DRITS V.A. (1977) Effectiveness of the electronometric method of measuring the intensities at the electron diffraction structural studies. *Izv. AN SSSR, Series Phys.* 2263–2271.

TSIPURSKY S.I., DRITS V.A. & CHEKIN S.S. (1978) Revealing of the structural ordering of nontronites by oblique texture electron diffraction. *Izv. AN SSSR, Ser. geol.* **10,** 105–113.

ZVYAGIN B.B. & PINSKER Z.G. (1949) Electron diffraction study of the montmorillonite structure. *Dokl. Acad. Nauk SSSR.* **68,** 30–35.

ZVYAGIN B.B. (1967) *Electron Diffraction Analysis of Clay Mineral Structures.* Plenum Press, New York.

ZVYAGIN B.B., VRUBLEVSKAYA Z.V., ZHOUKHLISTOV A.P., SIDORENKO O.V., SOBOLEVA S.V. & FEDOTOV A.F. (1979) In: *High Voltage Electron Diffraction Study of Layer Minerals* (V. A. Drits, editor). Nauka, Moscow.